Genetics: Early Online, published on January 3, 2018 as 10.1534/genetics.117.300571

An expanded role for the RFX transcription factor DAF-19, with dual functions in ciliated and non-ciliated neurons

Elizabeth A. De Stasio*, Katherine P. Mueller*[1], Rosemary J. Bauer*, Alexander J. Hurlburt*, Sophie A. Bice*, Sophie L. Scholtz*, Prasad Phirke[†], Debora Sugiaman-Trapman[†], Loraina A. Stinson*, Haili B. Olson*, Savannah L. Vogel*, Zabdiel Ek-Vazquez*, Yagmur Esemen*, Jessica Korzynski*, Kelsey Wolfe*, Bonnie N. Arbuckle*, He Zhang*, Gaelen Lombard-Knapp*, Brian P. Piasecki*, Peter Swoboda[†]

Affiliations:

*Department of Biology, Lawrence University, Appleton, WI 54911, USA

[†]Karolinska Institute, Department of Biosciences and Nutrition, 141 83 Huddinge, Sweden

[1]current address: Department of Biomedical Engineering and Wisconsin Institutes for Discovery, University of Wisconsin – Madison, WI 53715, USA

Microarray datasets were submitted to the Gene Expression Omnibus (GEO) database under accession number GSE96068.

Running Title: An expanded role for *daf-19*

Key Words: RFX transcription factor, neuronal gene expression, dauer formation, roaming behavior, aldicarb resistance

Corresponding Author:

Elizabeth A. De Stasio

Department of Biology

711 E. Boldt Way, SPC 24

Lawrence University

Appleton, WI, USA

920-832-7682 (office)

920-209-4701 (cell)

elizabeth.a.destasio@lawrence.edu

ABSTRACT

Regulatory Factor X transcription factors (RFX TFs) are best known for activating genes required for ciliogenesis in both vertebrates and invertebrates. In humans, eight RFX TFs have a variety of tissue-specific functions, while in the worm *Caenorhabditis elegans,* the sole RFX gene, *daf-19,* encodes a set of nested isoforms. Null alleles of *daf-19* confer pleiotropic effects including altered development with a dauer constitutive phenotype, complete absence of cilia and ciliary proteins, and defects in synaptic protein maintenance. We sought to identify RFX/*daf-19* target genes associated with neuronal functions other than ciliogenesis using comparative transcriptome analyses at different life stages of the worm. Subsequent characterization of gene expression patterns revealed one set of genes activated in the presence of DAF-19 in ciliated sensory neurons and whose activation requires the *daf-19c* isoform, also required for ciliogenesis. A second set of genes is down-regulated in the presence of DAF-19, primarily in non-sensory neurons. The human orthologs of some of these neuronal genes are associated with human diseases. We report the novel finding that *daf-19a* is directly or indirectly responsible for down-regulation of these neuronal genes in *C. elegans* by characterizing a new mutation affecting the *daf-19a* isoform (*tm5562*) and not associated with ciliogenesis, but which confers synaptic and behavioral defects. We have thus identified a new regulatory role for RFX TFs in the nervous system. The new *daf-19* candidate target genes we have identified by transcriptomics will serve to uncover the molecular underpinnings of the pleiotropic effects *daf-19* exerts on nervous system function.

INTRODUCTION

Characterizing Regulatory Factor X transcription factor (RFX TF) function and identifying RFX target genes are key to understanding a wide range of diseases. Problems with RFX-controlled genes are linked to impaired immune function, cancer, and ciliopathies including developmental disorders, kidney disease, and deafness. RFX TFs regulate processes including mitosis in yeasts (Garg et al., 2015), ciliogenesis and cilia maintenance (Choksi et al., 2014), adaptive immune responses (Reith and Mach, 2001), innate immunity (Xie et al., 2013), and maintenance of terminally differentiated hair cells in the mammalian ear (Elkon et al., 2015). RFX target genes encode ciliary components (*e.g.* Schafer et al., 2003; Jensen et al., 2016), phosphatases involved in carcinogenesis (Su et al., 2014), major histocompatibility complex genes (Meissner et al., 2012), and genes associated with dyslexia (Tammimies et al., 2016), to name a few.

RFX TFs share and are defined by a highly conserved winged helix DNA-binding domain (DBD) (Emery et al., 1996; Gajiwala et al., 2000) by which gene networks are regulated in both invertebrates and vertebrates. RFX TFs evolved early in the unikont lineage, and, though well known for controlling ciliogenesis, they apparently evolved after the origin of cilia (Chu et al. 2010; Piasecki et al., 2010). Thus they likely have an ancient function. Humans have eight RFX genes (Aftab et al., 2008; https://www.ncbi.nlm.nih.gov/gene/731220. RFX TFs regulate target genes via a highly conserved *cis*-acting regulatory sequence called the X-box motif (Efimenko et al. 2005; Laurencon et al. 2007; Chu et al., 2012). The X-box sequence has been used effectively to

identify many RFX target genes (*e.g.* Blacque et al., 2005; Chen et al., 2006; Henriksson et al. 2013).

Here we describe novel functions for *daf-19*, the only RFX gene in the worm *C. elegans*. DAF-19 was the first RFX TF linked to the process of ciliogenesis (Swoboda et al., 2000; Senti and Swoboda, 2008) and it was found also to regulate innate immunity (Xie et al., 2013). The *C. elegans daf-19* locus encodes at least four related gene products with three transcriptional start sites (Craig et al., 2013). Two smaller isoforms, DAF-19C and DAF-19M (Figure 1A), have a role in ciliated sensory neurons (CSNs) only. The majority of CSNs, the only ciliated cell type in the worm, are generated during embryogenesis (Jensen et al., 2016). *daf-19c*, expressed in all CSNs via an internal promoter (Senti and Swoboda, 2008; Craig et al., 2013), is sufficient to drive ciliogenesis in CSNs (Senti et al., 2009). DAF-19C alone is also sufficient to drive continued larval development in a food-rich environment as opposed to entering the dispersive and stress-resistant dauer larval stage (Senti and Swoboda, 2008). DAF-19C regulates transcription of ciliary genes via X-box motifs supported by a nearby C-box enhancer element (Burghoorn et al., 2012). In contrast, the *daf-19m* isoform is expressed only in IL2 and male-specific CSNs, where it regulates the transcription of genes required for male mating behaviors, including those with orthologs implicated in polycystic kidney disease (Wang et al., 2010). Gene regulation by DAF-19M results in cilia specialization via a DAF-19C-independent cascade of gene expression (Wang et al., 2010).

Roles for the larger DAF-19A/B isoforms extend into adulthood, including regulation of foraging behavior and synaptic protein maintenance (Senti and Swoboda, 2008). *daf-19a*

and *b* differ by one small, alternately spliced exon (Figure 1A-C), are highly expressed in non-ciliated neurons (Saito et al., 2013), and are also less highly expressed in the hypodermis and body wall muscle at all life stages (Senti and Swoboda, 2008; Craig et al., 2013). Null *daf-19(m86)* mutant adults expressing only transgenic DAF-19C have apparently normal cilia and sensory functions, but display abnormal dwelling and roaming behaviors (Senti and Swoboda, 2008), consistent with a synaptic defect in non-sensory neurons (Flavell et al., 2013). This defect was confirmed by pharmacological studies and a noted reduction in certain synaptic protein levels in adults. RNA levels of these proteins were not, however, similarly decreased (Senti and Swoboda, 2008) suggesting an indirect regulatory effect of DAF-19A/B on synaptic protein turnover. Thus, *daf-19* promotes certain neuronal functions beyond ciliogenesis at the embryonic life stage, and these pleiotropic effects can be attributed to downstream effects of different *daf-19*-regulated genes. We sought to identify new DAF-19 target genes, particularly DAF-19A target genes that function in neurons, by characterizing post-embryonic transcriptomes of *daf-19(m86)* null mutants and isogenic age-matched controls at the L1 larval and adult stages of development. Transcriptome approaches have previously successfully identified new RFX target genes expressed early in worm development (Chen et al., 2006; Phirke et al., 2011; Jensen et al., 2016) and in other organisms, including humans (*e.g.* Nelander et al., 2005; Wu et al., 2016).

We describe here for the first time target genes of DAF-19A, in addition to new target genes of DAF-19C. Further, we characterized a new *daf-19a/b* isoform-specific mutation (*tm5562*) and demonstrate that DAF-19A/B expression is directly or indirectly responsible for the down-regulation of target genes in certain non-sensory neurons, while DAF-19C

primarily activates genes in CSNs. We propose that the intricate interplay of DAF-19 isoforms controls the expression of different gene batteries in defined sets of neurons and that DAF-19 impacts neuronal functions ranging from basic synaptic maintenance to neuronal outputs in development (dauer formation) and behavior (foraging and locomotion).

MATERIALS AND METHODS

C. elegans strains and culture conditions

C. elegans strains (Table S1) were cultured at 20°C following standard procedures (Brenner, 1974) except for LU455, *daf-19(m86),* grown at 15° to obtain adults for behavioral assays. Gene expression studies at multiple life stages required the *daf-12(sa204)* allele to fully suppress the highly penetrant dauer formation constitutive (Daf-c) phenotype conferred by *daf-19(m86). him-5(e1490)* was used to generate males. The *daf-19(tm5562)* mutant was obtained from the Mitani lab collection and was out-crossed to wild-type N2 six times. Three primers [upstream (U), downstream (D), and poison (P)] identified the *tm5562* deletion allele during out-crossing: U5'AATGACCTTCACACGGTGTC, D5'CACACCGGGTGCTTCACCAT, P5'GCGCACAATAGGCTCCAAGC. The 865 bp deletion was confirmed by sequencing PCR amplicons after out-crossing. *daf-19(tm5562/+)* heterozygous and associated control animals were generated by mating to a strain carrying an integrated fluorescent marker.

L1 and adult stage worms were collected for transcriptome analysis from JT204 *daf-12(sa204)* and JT6924 *daf-19(m86); daf-12(sa204).* To collect L1 stage worms, worms were grown on agarose-containing solid egg-NGM medium for 6–7 days until a sizeable gravid adult worm population was observed. Embryos were isolated by hypochlorite treatment and grown to the 3-fold stage in S-Basal medium with *E. coli* OP50 with gentle agitation at 20°C. A second hypochlorite treatment removed hatched worms and dead eggs. Three-fold stage embryos were further grown on OP50 seeded NGM agarose plates for five hours to obtain

158 selectively enriched L1 stage worms. To obtain adult stage worms, a synchronized
159 hypochlorite-treated population was grown to the L4 stage on NGM agarose plates. Worms
160 were gently rinsed from plates and gravity-settled for 5 minutes, washed with M9 and settled
161 for three minutes, followed by a repetition with 1 minute of settling. Early-stage larvae and
162 embryos were left in each supernatant. This procedure was repeated after worms fed on
163 agarose media for another 24 hours. Two-day-old well-fed adults were harvested 50 hours
164 past the L4 stage.
165
166 **RNA extraction, cDNA preparation and labeling, microarray data generation**
167 Harvested worms were passed through three freeze and thaw cycles using liquid
168 nitrogen. For reverse transcriptase (RT) PCR and microarray analysis, total RNA from the L1
169 stage was isolated using a standard phenol-chloroform extraction procedure following
170 homogenization; total RNA from adults was prepared using TRIZOL followed by the Qiagen
171 RNAeasy kit following the manufacturer's directions. The quantity and quality of the
172 extracted RNA was determined using an Agilent Bioanalyzer 2100 (Agilent Inc, Santa Clara,
173 CA, USA). Standard eukaryotic target preparation protocol using 5μg of total RNA was
174 conducted for each array as described in the Affymetrix GeneChip Eukaryotic Sample
175 labeling protocol (Affymetrix Inc.). Four independent RNA preparations from L1 larvae and
176 three from adults of each strain were used for one GPL200 Affymetrix *C. elegans* genome
177 array hybridization each; array data were analyzed as described in the GeneChip Expression
178 Analysis technical manual (Affymetrix Inc.). *In vitro* transcription, fragmentation,
179 hybridization, staining, and scanning were performed by the Bioinformatics and Expression
180 Analysis core facility, Karolinska Institute, Stockholm-Huddinge, Sweden (www.bea.ki.se).

Primers for RT PCR analysis of *daf-19* were 5' GCCATCGACGAGCAGTGTG and 5' CATGCAAGGAGAGACGCTG. Additional primers for sequencing were 5' CTTACGAGGTGTTCCAGACGA, 5' TCGTCTGGAACACCTCGTAAG and 5' AGACGGATCGGATGAGCTTTC. RT PCR used the SuperScript III One-Step RT PCR system (Invitrogen).

Transcriptome analysis

Subsequent to scanning, microarrays were subjected to a range of low stringency analyses, including image analyses, signal summarization, and normalization. Expression reports were examined to confirm that all internal control values were within the acceptable range, as defined by the Affymetrix Data Analysis Fundamentals (Affymetrix, Inc). Data passing all quality control measures were utilized for further statistical analyses.

CEL files obtained from microarray hybridizations were imported into RMA Express (version 0.3; http://rmaexpress.bmbolstad.com) and expression signal values were calculated using a robust multichip average (RMA) expression summary and quantile normalization technique. BRB Array Tools (version 3.3; http://linus.nci.nih.gov/BRB-ArrayTools.html) were used to identify genes with statistically significant variation in expression. The probability threshold was set at a maximum of 0.05 (p-value $\leq$0.05) for genes to be considered statistically differentially expressed in wild-type and mutant populations. Genes with a signal variation of 1.5-fold or greater were selected for subsequent experiments. To reduce false discoveries, a class comparison test was conducted using a multivariate permutation test with a confidence level of 97% (L1 analysis) and 90% (adults). This analysis

revealed that 403 probes identified 370 unique differentially regulated genes (n=235 down-regulated and n=135 up-regulated) in *daf-19* mutant L1 larvae. Such a permutation is very similar to that utilized by the Significance Analysis of Microarrays (SAM) analyses (Tusher et al., 2001). Additional lists of genes were generated using SAM (version 2.2) with a false discovery rate (FDR) of less than or equal to 5% (Q-value ≤5%) for L1 analysis and 10% for adult analysis. Thirty repeated runs of SAM were performed using variable random seed numbers for each run. During each run of SAM, 100 permutations were performed. Probes appearing with a bootstrap frequency of 24 (80% of total runs) were further considered for signal variation filtering, used to selectively identify genes with a 1.5-fold or greater variation between the two genetic conditions (L1 larvae: n=154 down-regulated, n=58 up-regulated). The list of genes differentially regulated in adults was generated similarly: RMA normalization followed by class comparison with a multivariate permutation, a false discovery rate of 0.1 and 70% confidence level (n=120 down-regulated genes, n=75 up-regulated). SAM analysis yielded a list of 119 unique genes (n=74 down-regulated; n=45 up-regulated) that is completely contained within the larger list of differentially regulated genes. Comparisons between transcriptomes (3-fold stage embryos, Phirke et al., 2011; L1 larvae, this work; adults, this work) were undertaken using the gene lists generated by class comparison (Tables S2-S4).

Transcriptional GFP fusion-gene expression constructs

Gene expression was assessed exclusively using transcriptional GFP reporter constructs generated by inserting 1-3 kb of DNA upstream of genes of interest into the poly-cloning site of the GFP reporter plasmid pPD95.75 (Table S5). Germline transformations by

227 microinjection (Mello et al., 1991) used one of two methods. In one set, GFP constructs (40
228 ng/µl) and the co-transformation marker *elt-2p::mCherry* (10 ng/µl; gift from Gert Jansen;
229 Burghoorn et al., 2010) were micro-injected with carrier DNA at 50 ng/µl. Worms
230 expressing mCherry in the intestine were analyzed for GFP expression. Alternatively, GFP
231 constructs (70 ng/µl) were co-injected with 30ng/µl *unc-122p::DsRed* with no carrier DNA.
232 Worms with DsRed expression in coelomocytes were analyzed for GFP expression.
233 Transgene GFP expression patterns were characterized in no fewer than 30 L1-adult stage
234 worms per strain using a Leica TCS SP5 II confocal microscope; adult expression patterns
235 are shown. For *gakh-1* and *del-4* age-dependent expression analysis, N=130 and 40 per strain,
236 respectively. Worms were immobilized using 10mM NaN_3 on 2.0% agarose pads. Two *daf-*
237 *19* translational constructs fused isoform-specific endogenous promoters to partial cDNAs
238 expressing either *daf-19a* (pGG67_3) or *daf-19c* (pGG14) (described in Senti and Swoboda,
239 2008); these two constructs were used for isoform-specific rescue experiments.
240
241 **Dye-filling and behavioral assays**
242 Fluorescent dye-filling assays (Starich et al., 1995) using DiI (Molecular Probes)
243 were used to confirm cilia defects in *daf-19* mutant animals and to assist with neuronal
244 identification in wild-type worms.
245 Dauer formation assays: Twenty gravid hermaphrodites were placed on OP50 for six
246 hours and dauer larvae were enumerated after five days (15°), 4 days (20°) or 3 days (25°) of
247 growth. Tukey's pairwise comparisons of arcsine-transformed data were used to detect
248 differences in average dauer production between strains for three replicate experiments. All
249 behavioral and life history assays were done blind to strain identity.

Early life history: Thirty gravid hermaphrodites were placed on OP50 for two hours to produce tightly synchronized populations. The life stage of each offspring was assessed every eight hours. Tukey's pairwise comparisons were used to detect significant differences in percent of worms at particular life stages in three replicate experiments.

Roaming assays: L4 worms were grown on fresh OP50 lawns for 12 hours after which thirty adult worms were individually picked to the center of a bacterial lawn and allowed to forage for one hour at 19° and constant humidity. The proportion of OP50-covered 5 mm squares crossed by tracks was enumerated (cf. Senti and Swoboda, 2008). Replicate assays were repeated on seven different dates. Data were arcsine-transformed for statistical analysis. Two-way ANOVA analysis revealed assay date to be a significant variable; the behavior of each strain was compared using Tukey's pairwise comparisons for each assay date.

Aldicarb assays: Twenty hermaphrodites, 30 hours post-L4 stage, were placed on OP50 seeded NGM agar containing 500 μM aldicarb. Complete paralysis of the head was scored as in Mahony et al. (2006). Data from each of six replicate assays were compared using a survivorship curve comparison test (Pyke and Thompson, 1986).

Data availability

All microarray datasets were submitted to the Gene Expression Omnibus (GEO) database (Edgar and Barrett, 2006) under accession number GSE96068. *C. elegans* strains (Table S1) are available upon request. Gene lists generated from this study as well as from Phirke et al. (2011) are included in Tables S2-S4; Table S5 lists all the primers used and Table S6 lists transgene constructs with apparent DAF-19 independent expression.

RESULTS

Identification of DAF-19 target genes in L1 larvae and adult worms

To identify novel DAF-19 target genes we employed whole-genome microarrays of *daf-19(m86)* null mutants and isogenic wild-type worms from synchronized L1 larvae and 2-day old adults. To add to the comparably prepared gene lists from embryos (Chen et al., 2006; Phirke et al., 2011 in Table S2), a comparison of mutant and wild-type populations (cf. Materials and Methods) uncovered large sets of differentially regulated genes in L1 larvae (Table S3) and adult worms (Table S4).

We determined whether DAF-19 regulated transcriptomes were enriched for particular types of genes and whether that enrichment changed during development. We found that the breadth of gene categories represented by DAF-19 regulated transcriptomes narrowed as development proceeded from embryos to L1 stage larvae to adults (Table 1). Based on the timing of ciliogenesis, we expected that DAF-19 regulated transcriptomes from embyros and L1 larvae would be enriched for genes involved in ciliogenesis, while this would not be the case for the adult stage gene list. Such a finding would be consistent with the results from Jensen et al. (2016) who used a gene expression profiling approach to track ciliary gene expression during development. Our DAF-19 regulated transcriptome from L1 stage larvae was grouped into nine gene ontology clusters with enrichment scores >1.5 (Huang et al., 2009) each containing at least ten genes, including clusters representing cilia, dauer formation, signaling, and aging. By comparison, the DAF-19 regulated transcriptome from adults was enriched for smaller sets of genes involved in signaling, aging, and

proteolysis. Both of these transcriptomes displayed an even stronger reduction in clusters, when compared to the three-fold stage embryo DAF-19 regulated transcriptome (Phirke et al., 2011) (Tables 1 and S2).

Comparisons with the Cilia database CilDB (Arnaiz et al., 2014) also indicated an enrichment of known ciliary genes in the gene list from L1 larvae but not in the gene list from adults. Overall, CilDB identifies 15% of *C. elegans* genes as ciliary based on two or more published studies. Using the same criteria, we identified more than 21% of the gene list from L1 larvae as ciliary, while only 11% of the adult gene list were known ciliary genes. Core ciliary genes (*e.g. bbs* and *nphp* genes) important for the process of ciliogenesis (Choksi et al., 2014) were represented with statistical significance only on the gene lists from embyros and L1 larvae, indicating that the maintenance of cilia at the adult stage is very likely much less dependent on DAF-19 regulation. Lastly, there was significant enrichment (4-10 fold) in all three lists (3-fold stage embryo, L1 larvae, adults) for genes expressed in neurons, with expression patterns becoming more restrictive as development proceeds (Figure S1). In light of the suggested function of DAF-19A/B in regulating the maintenance of protein levels at neuronal synapses, we note the presence in the adult gene list of twelve genes involved in proteolysis (Table 1), three of which we characterized in more detail: *spg-20*, *anp-1*, and *skr-12*.

For further analyses we chose a number of genes based on one of the following criteria: (1) a suggested neuronal expression pattern, (2) a Wormbase annotation suggesting a connection to *daf-19* mutant phenotypes such as protein stability or innate immunity, or (3)

no known function or expression pattern (see Table S5). In total we assessed expression patterns of 44 candidate *daf-19* target genes using transcriptional GFP fusions, 32 of which have identified human orthologs (Shaye and Greenwald, 2011). Out of the 44 genes, 33 showed strong GFP expression that was characterized further, whereby expression patterns were always compared between isogenic strains differing only by the *daf-19* allele. Gene choices were not filtered for their presence in an operon; four such genes were analyzed, three that are the first gene of an operon and one, *ddn-1*, that was the second (based on Allen et al., 2011). Characteristics of *daf-19* target genes and their expression patterns are summarized in Tables 2 and S6.

The presence of DAF-19 activates gene expression

We compared the expression of putative target gene transcriptional fusions in *daf-19* null and wild-type genetic backgrounds to determine where and in which way target gene expression was DAF-19 dependent. Our transcriptome analysis revealed new genes activated in the nervous system in the presence of DAF-19. Seven gene promoter fusions showed clear evidence of activation by the presence of wild type DAF-19 in neurons, mostly limited to subsets of CSNs (Table 2). The inner labial (IL2) neurons were a common site of *daf-19* target gene activation; expression of *asic-2*, *spg-20*, and *ddn-1* (down-stream of *daf-19*) (Figure 2) as well as *ddn-2* (F35C5.11 in Phirke et al., 2011) and *mapk-15* (Piasecki et al., 2017) in IL2 neurons required *daf-19*. IL2 neuron identity was confirmed by co-localization with a *cho-1::mCherry* reporter (Pereira et al., 2015) or lack of co-localization with *eat-4::mCherry* (Serrano-Saiz et al., 2013) (Figure S2). *ddn-1::gfp* is also differentially expressed in other CSNs; we observed robust activation in the presence of DAF-19 in ASG,

342 less pronounced activation in URX (not a CSN), ASI, and AFD, the latter identified by *eat-4*
343 co-localization.
344
345 Even though DAF-19C is expressed in many or all CSNs and DAF-19A/B in nearly
346 all non-ciliated neurons (Senti and Swoboda, 2008), all *daf-19* target genes examined appear
347 to have RFX-independent expression in some neurons in addition to DAF-19 dependence in
348 a subset of neurons (Table 2). For example, robust expression of *spg-20::gfp* was observed in
349 the majority of neurons, but DAF-19-dependent activation was discernable only in IL2
350 neurons (Figure 2). Expression of *eppl-1::gfp* appeared DAF-19-dependent only in the CSNs
351 ASE and ASG (Figure 2), but not in PQR or non-neuronal tissues, while DAF-19-dependent
352 activation of *xbx-9::gfp*, found in our gene lists and previously described by Burghoorn et al.
353 (2012), was restricted to three of four CSNs in which expression was observed. Finally, *del-*
354 *4::gfp* expression was age-dependent in ASE, ASG, and several other unidentified neurons
355 (Figure 2 and Table 2). ASE and ASG were identified by location, morphology, and by
356 elimination: they do not dye-fill and are not cholinergic (Figure S2). In wild-type animals,
357 *del-4* expression decreased from eight amphid CSNs in L1-L2 larvae to half as many in
358 adults. In *daf-19(m86)* null mutant worms, no more than three neuron pairs expressed *del-4*
359 in young larvae and only one or two AIA neurons did so in adults. We conclude that DAF-19
360 activates *del-4* expression in ASE and in AIY interneurons. In other studies, *del-4* transcripts
361 were found in ASE following SAGE analysis and the gene contains an ASE motif
362 (Etchberger et al., 2007) as well as an X-box motif (Efimenko et al., 2005).
363
364 **DAF-19 presence down-regulates some genes in the nervous system**

Because two RFX orthologs in humans and yeast have been found to repress gene expression, we assessed expression patterns of several genes that appeared to be up-regulated in the absence of DAF-19 in our gene lists. For the first time, we report that wild type DAF-19 can down-regulate target gene expression in both ciliated and non-ciliated neurons. Three genes, all of which showed differential transcription in at least two life stages, were expressed in fewer neurons in wild-type worms than in *daf-19(m86)* null mutants. One additional gene, *mapk-15*, not identified by microarray analysis, was also down-regulated by DAF-19 (Table 2).

daf-19-dependent down-regulation of *skr-12* was seen in more than four sets of CSNs. Based on *eat-4* co-localization, we identified *skr-12* expression in the CSNs IL1, ASG, and AFD, and occasionally in the OLQ neurons in *daf-19(m86)* null mutants (Figures 3 and S2). The characteristic microvilli at the tip of the AFD dendrites (Doroquez et al., 2014) were easily visible (Figure 3). Expression in two other CSNs, most likely ASE and ADF, was also down-regulated by the presence of DAF-19. Two additional neurons in which *skr-12* was down-regulated could not be identified due to faint expression levels. Expression of *skr-12* in the ASI and ASK amphid CSNs (identified through co-localization with DiI) as well as in the intestine and pharyngeal muscle appeared to be *daf-19* independent.

daf-19 dependent down-regulation of *gakh-1* was observed consistently in non-ciliated neurons in an age-dependent manner. In wild-type adults, *gakh-1::gfp* was always expressed in the cholinergic RIF neurons and, rarely, in the AIY interneurons and the M4 pharyngeal motor neuron (Figures 3 and S2). In *daf-19(m86)* mutants, however, the

transgene was expressed in at least four additional sets of interneurons: AVB, AIY, AIN and AVA (both less frequently) and either the SIAD and SIAV interneurons or possibly the SMBD motor neurons (Figures 3 and S2). These latter neurons could not be unambiguously distinguished using *cho-1::mCherry* co-localization or by their morphology, but they never expressed *gakh-1* in wild-type worms (N=132). In L3 and younger larval *daf-19* mutants, additional neuronal expression was seen in the glutamatergic BAG CSNs and, at low levels, in *cho-1*-expressing neurons anterior to the nerve ring (Figure S2). Sieburth et al. (2005) also reported *gakh-1* expression in the intestine, pharynx, and head and tail neurons in wild-type worms.

Only in *daf-19* mutant worms, *rgs-8.1::gfp* was consistently expressed in the I2 pharyngeal and non-ciliated RID head neurons as well as less frequently in four neurons of the tail (Figures 3 and S2), including the PVQ interneuron pair, one of the DVA, B, or C neurons, and a single neuron directly posterior of PVQ. Expression in the PVT tail neuron was irregular in both wild-type and *daf-19* mutant backgrounds. *rgs-8.1* was also found to be differentially regulated in embryonic *daf-19(m86)* null mutant transcriptomes (Chen et al., 2006; Phirke et al., 2011).

In summary, expression of four target genes is down-regulated only in the presence of DAF-19. This down-regulation is specific to the nervous system.

Characterization of genes whose expression is (largely) independent of DAF-19

Fifteen gene promoter fusions yielded GFP expression in neurons that was (largely) independent of DAF-19 (Figure S3 and Table S6). This holds true also for genes expressed in both neurons and the intestine or for genes (predominantly) expressed in the intestine, where they might be involved in innate immunity (Xie et al., 2013) (Figure S3 and Table S6). Three genes, *anp-1*, *hex-1*, and C06G3.6, showed a clear reduction in the frequency of neuronal expression in a *daf-19(m86)* null mutant background (Table S6). Seven genes were expressed in the intestine and not the nervous system and another fourteen were expressed in both tissues. In no case could we detect *daf-19* dependent expression in the intestine (Table S6), even when neuronal expression was dependent on the presence of functional DAF-19 (N=5 genes; Table 2). Similarly, though *daf-19* has been reported to be expressed to some extent in body wall muscle and hypodermis (Senti and Swoboda, 2008), expression of target genes in either tissue was indistinguishable between wild type and *daf-19(m86)* null mutants (Table S6). Apparent DAF-19 independence of putative target gene expression could be due to incomplete control regions in our transcriptional fusion constructs, DAF-19 dependence only at embryonic stages of development that were not fully assessed, or false positives in the microarray data. Thus, our experiments revealed *daf-19* dependent target gene expression in the nervous system only.

Characterization of *tm5562*, an isoform-specific allele of *daf-19*

To determine which of the abundant DAF-19 isoforms (A or C) is responsible for controlling target gene expression, we characterized a new *daf-19* allele, *tm5562* (Figure 1). *tm5562* alters both *daf-19a* and *b* transcripts via deletion of exon 2, 582 bp of intron 1, and 93 bp of intron 2. RT PCR revealed that *tm5562* mutant worms produced RNAs shorter than

433 wild type by the predicted length of exon 2 (Figure 1B). Both *daf-19a*, in which exon 3 is
434 spliced to exon 5, and the *daf-19b* isoform including exon 4, were affected (Figures 1B-D).
435 Only in RNA isolated from *tm5562* mutants was exon 1 perfectly spliced to exon 3 in both
436 isoforms (Figure 1D). Sequencing of RT PCR amplicons as well as of genomic DNA
437 revealed no other mutations through the DNA binding domain (data not shown). The *tm5562*
438 transcript is expected to produce in-frame proteins lacking the evolutionarily conserved exon
439 2 (Figure 1E).
440
441 We determined that *daf-19(tm5562)* confers phenotypes expected of a *daf-19a* but not
442 a *daf-19c* mutant, such as roaming and pharmacological defects previously reported (Senti
443 and Swoboda; 2008). Wild-type worms will both dwell in small areas of a bacterial lawn and
444 will roam to (Ben Arous et al., 2009), or explore (Flavell et al., 2013), new areas. We
445 quantified the roaming behavior of individual worms and detected significant difference
446 between strains (Figures 4A and B). *daf-19(tm5562)* worms displayed less roaming behavior
447 than did wild-type N2 worms on all seven assay dates ($p<0.003$). In all assays, *daf-*
448 *19(tm5562)* behavior was either indistinguishable from that of *daf-19(m86)* null mutants (p
449 >0.5) or displayed an intermediate phenotype, statistically distinguishable from both wild-
450 type N2 ($p<0.002$) and *daf-19(m86)* null mutants ($p<0.02$). As was the case for *daf-19(m86)*
451 (Senti and Swoboda, 2008), the aberrant roaming behavior of *daf-19(tm5562)* worms was
452 rescued by transgenic expression of a *daf-19a*-specific construct ($p<0.03$) (Figure 4B).
453
454 We assessed synaptic function in *daf-19(tm5562)* mutants using resistance to aldicarb,
455 a cholinesterase inhibitor. For comparison, *daf-19(m86)* one-day old adult worms were

consistently resistant to aldicarb, though not to the level of age-matched *unc-29(e1072)* mutants lacking a subunit of the acetylcholine receptor (Figure 4C). Age-matched *daf-19(tm5562)* worms were resistant to aldicarb at levels statistically indistinguishable from those of *daf-19(m86)* worms in an average of six replicate assays (p=0.56). This synaptic defect was rescued by transgenic expression of *daf-19a* (p=0.02). Average aldicarb sensitivity of rescued worms was indistinguishable from that of wild-type N2 (p=0.56) (Figure 4C).

We used the aldicarb assay to test whether *daf-19(tm5562)* is a hypermorphic or dominant negative allele. If so, we expect heterozygous *tm5562/+* mutant animals to confer an aldicarb resistant phenotype. Instead, we found that *daf-19(tm5562/+)* heterozygotes had a phenotype indistinguishable from that of wild-type N2 worms mated with the same fluorescently marked strain (Figure S4D) (cf. Materials and Methods). We conclude that *daf-19(tm5562)* is a hypomorphic or loss-of-function allele affecting both *daf-19a* and *b* isoforms.

As expected, the *tm5562* allele did not appear to affect *daf-19c* function. While the *daf-19(m86)* null allele confers a highly penetrant dauer constitutive (Daf-c) phenotype (Swoboda et al., 2000), *daf-19(tm5562)* did not confer a Daf-c phenotype in the presence of food at any temperature tested (Figure S4A). Normal progression from the first to second larval stages thus indicates that *daf-19a/b* is not responsible for the developmental decision to enter the dauer larval stage. Animals lacking DAF-19C do not develop cilia and therefore CSNs that normally take up the fluorescent, lipophilic DiI can no longer do so. The fact that *daf-19(tm5562)* worms dye-filled normally in both amphids (Figure S4B) and phasmids (not

shown), and males mated readily with hermaphrodites suggests normal cilia development. These phenotypes are consistent with expression of functional *daf-19c* transcripts in *daf-19*(*tm5562)* worms.

Because *daf-19* can affect development, we followed worm development in populations synchronized by a two-hour time window (Figure S4C). We found that *daf-19(tm5562)* worms developed more slowly through the L3 stage, as indicated by the larger number of worms at this larval stage at 40 and 48 hours post-egg-lay ($p=0.00023$ as compared to wild-type N2). We conclude that the time course of larval development of *daf-19(tm5562)* worms was slightly altered. Similar phenotypes, notably an L2 stage extension, have been found for Daf-c temperature sensitive mutants of *daf-2*, when at the permissive temperature these worms do not enter the dauer stage (Ruaud et al., 2011; Olmedo et al., 2015). In summary, phenotypes conferred by *daf-19(tm5562)* are consistent with those of *daf-19(m86)* null mutant worms in which the *daf-19c* isoform is rescued by transgene expression (Senti and Swoboda, 2008). These results indicate that the *tm5562* allele strongly reduces or eliminates solely the function of the longer *daf-19a* and *b* isoforms (cf. Figure 1A). Rescue of *tm5562* phenotypes by *daf-19a* expression suggests that DAF-19A plays an important and unique role in nervous system function.

daf-19 isoform-specific regulation of target gene expression

We used the *daf-19(tm5562)* genetic background to determine whether differential target gene expression required functional DAF-19A. For six target genes for which the presence of DAF-19 activated expression, we compared the expression patterns between *daf-*

19(tm5562) mutants and *daf-19(m86)* null mutant worms that carried isoform-specific rescuing transgenes [notated as *daf-19(0)+a* or *+c*]. With no exceptions, these six target genes remained activated in a *daf-19(tm5562)* background (Figure 5 and Table 3). Consistent with this finding, the activated expression of these six target genes was rescued in *daf-19(0)+c* animals, whereas in *daf-19(0)+a* animals it was not rescued. Surprisingly, transgenic over-expression of *daf-19a* repressed the near-pan-neuronal expression of *spg-20* as well as all expression of *asic-2* (Figure 5), a phenotype we term *ectopic repression* (Table 3).

In contrast, down-regulation of target genes appeared to depend primarily, but not exclusively, on the action of DAF-19A. In *daf-19(tm5562)* mutant worms *skr-12* and *gakh-1* were highly expressed; that is, they were not repressed in a *daf-19a* mutant background, but they were repressed in an isogenic wild-type background (Figure 5 and Table 3). Over-expression of *daf-19c* did not change this lack of repression of *gakh-1* and, usually, *skr-12.* In a few animals, *skr-12* was repressed such that expression was limited to the ASE neurons (Figure 5). Over-expression of *daf-19a* fully rescued repression of *gakh-1,* yielding gene expression patterns exactly like that seen in wild-type worms, while repression of *skr-12* expression by the presence of DAF-19A was more extensive than the wild-type pattern (Figures 3 and 5). Thus, *skr-12* and *gakh-1* repression depended on functional DAF-19A.

To our surprise, *rgs-8.1* expression in I2 and RID neurons could be repressed in the presence of either isoform of DAF-19. Expression in I2 and RID and in tail neurons was repressed in *daf-19(tm5562)* worms as well as in both *daf-19(0)+a* and *+c* worms. These data suggest that a particular stoichiometry of DAF-19 proteins is important for the correct

expression of *rgs-8.1*. Note that in all cases, transgene presence was ascertained by the presence of the corresponding co-injection marker (cf. Materials and Methods and Figure 5). Lastly, a parallel project revealed that a kinase gene, *mapk-15*, appeared to be both activated and repressed by the presence of DAF-19. In the presence of DAF-19, *mapk-15* is activated in IL2, PHA, and PHB, and many male tail CSNs, but is partially down-regulated in IL1s and some of the neurons in the male tail (Piasecki et al., 2017). Expression in other CSNs, including many amphid head and the PQR tail CSNs does not depend on DAF-19. We found *mapk-15* activation in *daf-19(tm5562)* and in *daf-19(0)+c* worms, but not in *daf-19(0)+a* worms. Instead, over-expression of *daf-19a* repressed nearly all *mapk-15* expression in the head, with variable repression in the hermaphrodite tail and no repression in the male tail, again suggesting that DAF-19 stoichiometry is important for correct gene expression in some neurons.

We conclude with the novel finding that expression of the DAF-19A isoform down-regulates certain target genes in non-sensory neurons, while DAF-19C expression generally activates genes in CSNs and can, albeit rarely and restricted to small sets of neurons, also down-regulate gene expression. These results are consistent with the described, mutually exclusive expression patterns of these two DAF-19 isoforms (Senti and Swoboda, 2008).

DISCUSSION

Using comparative transcriptomics during different life stages of the worm *C. elegans* we have uncovered large sets of new target genes for DAF-19, the sole RFX TF in this organism. We can assign a number of these target genes to act in defined sets of neurons and, for some, at certain time points during development. DAF-19 dependent expression of these target genes extends beyond CSNs and the three-fold stage of embryogenesis, by which time most cilia are formed (Sulston et al., 1983; Nechipurenko et al., 2016). Our work thereby greatly expands the suggested roles for DAF-19 and its target genes beyond a role in ciliogenesis (Choksi et al., 2014). Specifically, the presence of the larger DAF-19A isoform down-regulates target genes in non-ciliated neurons in larval through adult stages, while the smaller DAF-19C isoform primarily activates target genes in particular subsets of CSNs. Thus, *daf-19* provides important contributions to the regulation and maintenance of neuron function throughout development and adulthood.

To determine which DAF-19 isoform regulates target gene expression, we characterized a novel *daf-19* allele, *tm5562,* a deletion of exon 2. The homozygous mutant confers neuronal phenotypes expected of a *daf-19a* mutant, e.g. dwelling/roaming defects and aldicarb resistance, but does not affect ciliogenesis or confer abnormal dauer development as expected of a *daf-19c* mutation. Since *daf-19(tm5562)* lacks exon 2 and acts as a loss-of-function allele, we suggest that amino acids encoded by this exon play an important role in DAF-19A function. Sequence alignment of available *daf-19* orthologs in different *Caenorhabditis* species reveals a highly conserved block of 22 amino acids (Figure

1E) in exon 2. Conservation of this sequence ranges from 80-90%. The conserved sequence is rich in positively charged amino acids but contains no currently recognized protein motif.

DAF-19 dependent down-regulation of neuronal gene expression in *C. elegans* is a newly described phenomenon. We identified new target genes, *skr-12*, *gakh-1*, *rgs-8.1*, and the recently characterized *mapk-15* (Piasecki et al., 2017), whose expression was down-regulated by DAF-19A in a subset of neurons. In another study, down-regulation by *daf-19* was reported for the gene *peli-1*, but only when a canonical proximal X-box promoter motif was removed and a less conserved, more distal X-box remained (Chu et al., 2012). None of the three down-regulated genes identified in our transcriptomics approach harbor an identified, canonical X-box promoter motif, while the *mapk-15* gene has a putative X-box motif (Blacque et al. 2005) located further upstream than is typical (Burghoorn et al., 2012; Piasecki et al., 2017). To what extent down-regulation of target genes by *daf-19* depends on X-box motifs, protein binding partners, or possible indirect effects will be subject of future studies.

RFX TFs have been found to repress target gene expression in other organisms. Human RFX1 is capable of auto-repression regulated by DNA damage and replication blocking (Lubelsky et al., 2005). Yeast RFX, Crt1, is also a transcriptional repressor that can repress its own promoter and that of other genes (Huang et al., 1998). Similar regulatory pathways control repression by these proteins in both humans and yeast (Lubelsky et al., 2005). *C. elegans* DAF-19 is most similar to human RFX1-4 (Choksi et al., 2014). The finding that DAF-19A expression down-regulates or represses target genes is thus conserved,

589 even if the biological pathways in which the respective RFX TFs act may differ. It will be of
590 interest to know whether target gene repression is linked to neuronal identity as described by
591 Hobert (2010).
592
593 Activation of target gene expression was shown to require the shorter DAF-19C
594 isoform, known to be necessary for ciliogenesis. Target gene activation is known to be
595 mediated through a canonical *cis*-acting X-box promoter motif (Blacque et al., 2005;
596 Efimenko et al., 2005; Chen et al., 2006), as well as a nearby C-box enhancer element
597 (Burghoorn et al., 2012). However, we found that four of the eight genes that were activated
598 by the presence of DAF-19C do not contain a canonical X-box. Though this finding is novel
599 for target genes activated by DAF-19C, Wang et al. (2010) found that DAF-19M target genes
600 lack a canonical X-box and Xie et al. (2013) found that an isoform of *daf-19* activates the
601 gene *tph-1* in the ADF neurons and antimicrobial genes in the intestine through an X-box
602 independent mechanism. These authors suggest that either DAF-19 regulates these target
603 genes through a different DNA sequence motif, an unrecognized degenerate X-box, or by
604 partnering through its dimerization domain with another transcription factor. Given that *daf-*
605 *19* lacks an apparent transcription factor activation domain, the latter model appears likely.
606 The fact that DAF-19 works with ATF-7 to regulate responses to pathogenic bacteria (Xie et
607 al., 2013) lends further support to such a model. Alternatively, regulation of target genes that
608 lack X-box motifs could be due to indirect effects of DAF-19C regulating other genes.
609
610 ***daf-19* alters gene expression in dauer-inhibiting and labial neurons**

611 Mutations in transcription factor genes often phenocopy neuronal ablation by causing
612 misregulation of target genes, thereby affecting specific neuron function (Hobert, 2016a).
613 *daf-19* null mutants are dauer formation constitutive, thus one might expect to see differential
614 gene regulation in neurons that inhibit dauer entry. Bargmann and Horvitz (1991) identified
615 the ADF, ASI, and ASG neurons as repressing dauer development in non-inducing
616 conditions. Conversely the ASJ neurons are required for initiating dauer development
617 (Schackwitz et al. 1996). Thus, we might expect to find DAF-19C-regulated gene expression
618 in ADF, ASI, ASG, but not in ASJ. We found that *ddn-1*, *eppl-1*, and *del-4* were strongly
619 activated by the presence of DAF-19C in ASG, *ddn-1* was weakly activated by DAF-19C in
620 ASI, and *skr-12* expression was down-regulated in ADF (Table 4) while none of the *daf-19*
621 regulated genes studied here were differentially expressed in ASJ neurons. It will be of
622 interest to determine whether any genes regulated by *daf-19* in this set of neurons are integral
623 to the inhibition of dauer entry.
624
625 In addition, a large number of genes are regulated by *daf-19* in the labial neurons
626 (Burghoorn, et al., 2012; this study), known to generate dendritic arbors in dauer larvae and
627 to direct dauer-specific behaviors (Schroeder et al., 2013). This suggests further work could
628 determine whether DAF-19 is one of the terminal selectors of labial neuron identity (cf.
629 Hobert, 2016b) as continued gene regulation in these neurons into adulthood suggests.
630
631 **_daf-19_-dependent gene regulation in neurons involved in foraging and locomotion**
632 Mutations in either major *daf-19* isoform are associated with aberrant roaming
633 behavior, specifically over-dwelling and increased turning based on observed worm tracks

(Figure 4; Senti and Swoboda, 2008). Thus, one might predict that *daf-19* target gene regulation would occur in neurons that inhibit dwelling and turning or that stimulate roaming. That is, neurons, which upon ablation, lead to increased dwelling and reduced exploration would be expected to express DAF-19-dependent genes. These neurons include ASI and AIY, required to suppress reversals and turns associated with the local search state and dispersal (Gray et al., 2005; Cohen et al., 2009); and the ASE, ASI, and BAG neurons that function in adaptive food leaving behavior when food is depleted (Milward et al., 2011). In contrast, one would not expect to see *daf-19*-dependent gene expression in HNS or NSM in which *tph-1* is responsible for suppressing exploration (Flavell et al., 2013).

We found differential expression of *daf-19* target genes in neurons that both induce exploration and suppress dwelling behaviors. *ddn-1* and *del-4* were activated in the ASI and AIY neurons, respectively. Three genes were activated in the ASE neurons, while *gakh-1* was repressed by *daf-19a* expression in the BAG neurons in larvae (Table 4). As predicted, we did not observe target gene regulation in HNS or NSM.

daf-19 regulates genes involved in protein homeostasis

We hypothesized that misregulation of genes involved in protein homeostasis contributes to neuronal phenotypes of adult *daf-19(m86)* mutants, based on detectable synaptic protein loss in these animals (Senti and Swoboda, 2008). Vayndorf et al. (2016) also demonstrated that neuron remodeling during aging is modified by compromised protein homeostasis. Gene ontology analysis of the differential transcriptome of adult worms (Tables 1 and S4) yielded an over-representation of putative *daf-19* target genes with designations of

ubiquitin and proteolysis. Of the 12 genes so identified, nine encode proteases or orthologs of the ubiquitin ligase system (http://www.wormbase.org). We analyzed expression patterns of three of these nine genes and found misregulation of all three in *daf-19* mutant backgrounds. *skr-12* is one of five SKP-1 ubiquitin ligase component orthologs (Edwards et al., 2009) in our adult differential transcriptome and it is down-regulated by DAF-19A, while *spg-20* encodes an ortholog of human SPG20, a ubiquitin ligase component implicated in spastic paraplegia (Karlsson et al., 2014), which is activated by the presence of DAF-19C. We also observed partial DAF-19-dependent activation of *anp-1*, which encodes an aminopeptidase (Table S6). In addition, Chu et al., (2012) reported that DAF-19 regulates *peli-1*, which encodes a protein with similarity to an E3 ubiquitin ligase. Modulation of *peli-1* expression (Huang et al., 2002) is consistent with neuronal phenotypes associated with worms lacking only DAF-19A, while *spg-20* mutants display lower crawling and thrashing speeds and are more sensitive to paraquat (Truong et al., 2015). In the future it will be of interest to determine whether mutations of these or other ubiquitin components alter synaptic protein homeostasis.

The work described here, along with that reported by Chen et al. (2006), Phirke et al. (2011) and Jensen et al. (2016), provides an exhaustive list of novel *daf*-19 target genes at four points during worm development: from embryogenesis to the adult stage. We have characterized orthologs of human disease genes, including *spg-20* (SPARTIN), mutations of which cause a spastic paraplegia called Troyer syndrome in humans (Patel et al., 2002), and *gakh-1*, encoding a possible regulator of clathrin-mediated membrane trafficking. Mutations of an orthologous human GAK gene are implicated in susceptibility to Parkinson's disease

(Pankratz et al., 2009; Hamza et al., 2010). These two examples, but also others from our gene lists, will aid in studies of neuronal function and in understanding connections to human disease. Lastly, our discovery that DAF-19, the sole *C. elegans* RFX transcription factor, modulates gene expression in non-ciliated neurons, opens up new avenues of research into the specification and function of non-sensory neurons.

Acknowledgements

Some worm strains were provided by the CGC, funded by NIH ($P4^0$ OD010440). We gratefully acknowledge online resources, particularly WormBase and WormAtlas. EAD was supported in this work by the NIH (R15AG16192-01), and by a Fulbright Research Fellowship with Sweden. An NSF-MRI grant (DBI-1126711) to EAD, BPP, and colleagues provided a confocal microscope. Undergraduate summer stipends were provided by NSF-WiscAMP (402549) and Lawrence University. Additional undergraduate students made contributions to this work: Kristen Bischel, Elisa Carloni, Christina Schaupp, and Lu Yu. EAD thanks Bart De Stasio for statistical expertise and moral support and the lab of Maureen Barr for a quiet place to write and wonderful colleagues, particularly Juan Wang for assistance with RT PCR. Work in the laboratory of PS was supported by the Swedish Research Council, and by the Marcus Borgström, Torsten Söderberg and Åhlén Foundations. PS also received support from the Swedish Foundation for Strategic Research and the Karolinska Institute (KI) Strategic Neurosciences Program. DST received support from the KI in the form of a PhD student (KID) scholarship.

LITERATURE CITED

Aftab, S., L. Semenec, J. S. Chu and N. Chen, 2008 Identification and characterization of novel human tissue-specific RFX transcription factors. BMC Evolutionary Biology **8:** 226.

Allen, M. A., L. W. Hillier, R. H. Waterston, T. Blumenthal, 2011 A global analysis of C. elegans trans-splicing. Genome Res. **21**:255.

Altun, Z. F., L. A. Herndon, C. A. Wolkow, C. Crocker, R. Lints *et al.*, 2002-2017 Wormatlas.

Angeles-Albores, D., R. Y. N. Lee, J. Chan and P. W. Sternberg, 2016 Tissue enrichment analysis for *C. elegans* genomics. BMC Bioinformatics **17:** 366.

Arnaiz, O., J. Cohen, A. Tassin and F. Koll, 2014 Remodeling Cildb, a popular database for cilia and links for ciliopathies. Cilia **3:** 9-9.

Bargmann, C. I., and H. R. Horvitz, 1991 Control of larval development by chemosensory neurons in *Caenorhabditis elegans*. Science (New York, N.Y.) **251:** 1243-1246.

Ben Arous, J., S. Laffont and D. Chatenay, 2009 Molecular and sensory basis of a food related two-state behavior in *C. elegans*. PloS one **4:** e7584.

Blacque, O. E., E. A. Perens, K. A. Boroevich, P. N. Inglis, C. M. Li *et al*, 2005 Functional genomics of the cilium, a sensory organelle. Current Biology **15:** 935-941.

Brenner, S., 1974 The genetics of *Caenorhabditis elegans*. Genetics **77:** 71-94.

719 Burghoorn, J., B. P. Piasecki, F. Crona, P. Phirke, K. E. Jeppsson *et al*, 2012 The *in vivo*
720 dissection of direct RFX-target gene promoters in *C. elegans* reveals a novel *cis*-regulatory
721 element, the C-box. Dev. Biol. **368:** 415-426.

722 Burghoorn, J., M. P. J. Dekkers, S. Rademakers, T. de Jong, R. Willemsen *et al*, 2010 Dauer
723 pheromone and G-protein signaling modulate the coordination of intraflagellar transport
724 kinesin motor proteins in *C. elegans*. J. Cell. Sci. **123:** 2076-2083.

725 Chen, N., A. Mah, O. E. Blacque, J. Chu, K. Phgora *et al*, 2006 Identification of ciliary and
726 ciliopathy genes in *Caenorhabditis elegans* through comparative genomics. Genome
727 Biol. **7:** R126.

728 Choksi, S. P., G. Lauter, P. Swoboda and S. Roy, 2014 Switching on cilia: Transcriptional
729 networks regulating ciliogenesis. Development **141:** 1427-1441.

730 Chu, J. S. C., M. Tarailo-Graovac, D. Zhang, J. Wang, B. Uyar *et al*, 2012 Fine tuning of
731 RFX/DAF-19-regulated target gene expression through binding to multiple sites in
732 *Caenorhabditis elegans*. Nucleic Acids Res. **40:** 53-64.

733 Chu, J. S. C., D. L. Baillie and N. Chen, 2010 Convergent evolution of RFX transcription
734 factors and ciliary genes predated the origin of metazoans. BMC Evolutionary
735 Biology **10:** 130.

736 Cohen, M., V. Reale, B. Olofsson, A. Knights, P. Evans *et al*, 2009 Coordinated regulation of
737 foraging and metabolism in *C. elegans* by RFamide neuropeptide signaling. Cell
738 Metabolism **9:** 375-385.

739 Craig, H. L., J. Wirtz, S. Bamps, C. T. Dolphin and I. A. Hope, 2013 The significance of
740 alternative transcripts for *Caenorhabditis elegans* transcription factor genes, based on
741 expression pattern analysis. BMC Genomics **14:** 249.

742 Di Tommaso, P., S. Moretti, I. Xenarios, M. Orobitg, A. Montanyola *et al*, 2011 T-coffee: A
743 web server for the multiple sequence alignment of protein and RNA sequences using
744 structural information and homology extension. Nucleic Acids Res. **39:** W13-W17.

745 Doroquez, D. B., C. Berciu, J. R. Anderson, P. Sengupta and D. Nicastro, 2014 A high-
746 resolution morphological and ultrastructural map of anterior sensory cilia and glia in
747 *Caenorhabditis elegans*. eLife **3:** e01948.

748 Edgar, R., and T. Barrett, 2006 NCBI GEO standards and services for microarray data. Nat.
749 Biotechnol. **24:** 1471-1472.

750 Edwards, T. L., V. E. Clowes, H. T. H. Tsang, J. W. Connell, C. M. Sanderson *et al*, 2009
751 Endogenous spartin (SPG20) is recruited to endosomes and lipid droplets and interacts with
752 the ubiquitin E3 ligases AIP4 and AIP5. Biochem. J. **423:** 31-39.

753 Efimenko, E., K. Bubb, H. Y. Mak, T. Holzman, M. R. Leroux *et al*, 2005 Analysis of xbx
754 genes in *C. elegans*. Development **132:** 1923-1934.

755 Elkon, R., B. Milon, L. Morrison, M. Shah, S. Vijayakumar *et al*, 2015 RFX transcription
756 factors are essential for hearing in mice. Nature Communications **6:** 8549.

757 Emery, P., B. Durand, B. Mach and W. Reith, 1996 RFX proteins, a novel family of DNA
758 binding proteins conserved in the eukaryotic kingdom. Nucleic Acids Res. **24:** 803-807.

759 Etchberger, J. F., A. Lorch, M. C. Sleumer, R. Zapf, S. J. Jones *et al*, 2007 The molecular
760 signature and cis-regulatory architecture of a *C. elegans* gustatory neuron. Genes
761 Dev. **21:** 1653-1674.

762 Flavell, S. W., N. Pokala, E. Z. Macosko, D. R. Albrecht, J. Larsch *et al*, 2013 Serotonin and
763 the neuropeptide PDF initiate and extend opposing behavioral states in *C. elegans*.
764 Cell **154:** 1023-1035.

765 Gajiwala, K. S., H. Chen, F. Cornille, B. P. Roques, W. Reith *et al*, 2000a Structure of the
766 winged-helix protein hRFX1 reveals a new mode of DNA binding. Nature **403:** 916-921.

767 Garg, A., B. Futcher and J. Leatherwood, 2015 A new transcription factor for mitosis: In
768 *Schizosaccharomyces pombe*, the RFX transcription factor Sak1 works with forkhead factors
769 to regulate mitotic expression. Nucleic Acids Res. **43:** 6874-6888.

770 Gray, J. M., J. J. Hill and C. I. Bargmann, 2005 A circuit for navigation in *Caenorhabditis*
771 *elegans*. Proc. Natl. Acad. Sci. U. S. A. **102:** 3184-3191.

772 Hamza, T. H., C. P. Zabetian, A. Tenesa, A. Laederach, J. Montimurro *et al*, 2010 Common
773 genetic variation in the HLA region is associated with late-onset sporadic Parkinson's
774 disease. Nat. Genet. **42:** 781-785.

775 Henriksson, J., B. P. Piasecki, K. Lend, T. R. Burglin and P. Swoboda, 2013 Finding ciliary
776 genes: A computational approach. Cilia, Pt B **525:** 327-350.

777 Hobert, O., 2010 Neurogenesis in the nematode *Caenorhabditis elegans*. WormBook.

778 Hobert, O., 2016a A map of terminal regulators of neuronal identity in *Caenorhabditis*
779 *elegans*. Wiley Interdisciplinary Reviews-Developmental Biology **5:** 474-498.

780 Hobert, O., 2016b Terminal selectors of neuronal identity. Essays on Developmental
781 Biology, Pt a **116:** 455.

782 Hobert, O., I. Carrera and N. Stefanakis, 2010 The molecular and gene regulatory signature
783 of a neuron. Trends Neurosci. **33:** 435-445.

784 Huang, D. W., B. T. Sherman and R. A. Lempicki, 2009 Systematic and integrative analysis
785 of large gene lists using DAVID bioinformatics resources. Nature Protocols **4:** 44-57.

786 Huang, M., Z. Zhou and S. J. Elledge, 1998 The DNA replication and damage checkpoint
787 pathways induce transcription by inhibition of the Crt1 repressor. Cell **94:** 595-605.

788 Huang, N. N., D. E. Mootz, A. J. M. Walhout, M. Vidal and C. P. Hunter, 2002 MEX-3
789 interacting proteins link cell polarity to asymmetric gene expression in *Caenorhabditis*
790 *elegans*. Development **129:** 747-759.

791 Jensen, V. L., S. Carter, A. A. W. M. Sanders, C. Li, J. Kennedy *et al*, 2016 Whole-organism
792 developmental expression profiling identifies RAB-28 as a novel ciliary GTPase associated
793 with the BBSome and intraflagellar transport. PLoS genetics **12:** e1006469.

794 Karlsson, A. B., J. Washington, V. Dimitrova, C. Hooper, A. Shekhtman *et al*, 2014 The role
795 of spartin and its novel ubiquitin binding region in DALIS occurrence. Mol. Biol.
796 Cell **25:** 1355-1365.

797 Laurencon, A., R. Dubruille, E. Efimenko, G. Grenier, R. Bissett *et al*, 2007 Identification of
798 novel regulatory factor X (RFX) target genes by comparative genomics in drosophila species.
799 Genome Biol. **8:** R195.

800 Lubelsky, Y., N. Reuven and Y. Shaul, 2005 Autorepression of rfx1 gene expression:
801 Functional conservation from yeast to humans in response to DNA replication arrest. Mol.
802 Cell. Biol. **25:** 10665-10673.

803 Mahoney, T. R., S. Luo and M. L. Nonet, 2006 Analysis of synaptic transmission in
804 *Caenorhabditis elegans* using an aldicarb-sensitivity assay. Nature Protocols **1:** 1772-1777.

805 Meissner, T. B., Y. Liu, K. Lee, A. Li, A. Biswas *et al*, 2012 NLRC5 cooperates with the
806 RFX transcription factor complex to induce MHC class I gene expression. Journal of
807 Immunology **188:** 4951-4958.

808 Mello, C. C., J. M. Kramer, D. Stinchcomb and V. Ambros, 1991 Efficient gene transfer in
809 *C. elegans*: Extrachromosomal maintenance and integration of transforming sequences.
810 EMBO J. **10:** 3959-3970.

811 Milward, K., K. E. Busch, R. J. Murphy, M. de Bono and B. Olofsson, 2011 Neuronal and
812 molecular substrates for optimal foraging in *Caenorhabditis elegans*. Proc. Natl. Acad. Sci.
813 U. S. A. **108:** 20672-20677.

814 Nechipurenko, I. V., A. Olivier-Mason, A. Kazatskaya, J. Kennedy, I. G. McLachlan *et al*,
815 2016 A conserved role for girdin in basal body positioning and ciliogenesis. Developmental
816 Cell **38:** 493-506.

817 Nelander, S., E. Larsson, E. Kristiansson, R. Mansson, O. Nerman *et al*, 2005 Predictive
818 screening for regulators of conserved functional gene modules (gene batteries) in mammals.
819 BMC Genomics **6:** 68.

820 Olmedo, M., M. Geibel, M. Artal-Sanz and M. Merrow, 2015 A high-throughput method for
821 the analysis of larval developmental phenotypes in *Caenorhabditis elegans*.
822 Genetics **201:** 443-448.

823 Pankratz, N., J. B. Wilk, J. C. Latourelle, A. L. DeStefano, C. Halter *et al*, 2009 Genome-
824 wide association study for susceptibility genes contributing to familial Parkinson Disease.
825 Hum. Genet. **124:** 593-605.

826 Patel, H., H. Cross, C. Proukakis, R. Hershberger, P. Bork *et al*, 2002 SPG20 is mutated in
827 Troyer Syndrome, an hereditary spastic paraplegia. Nat. Genet. **31:** 347-348.

828 Pereira, L., P. Kratsios, E. Serrano-Saiz, H. Sheftel, A. E. Mayo *et al*, 2015 A cellular and
829 regulatory map of the cholinergic nervous system of *C. elegans.* eLife **4:** .

830 Phirke, P., E. Efimenko, S. Mohan, J. Burghoorn, F. Crona *et al*, 2011 Transcriptional
831 profiling of *C. elegans* DAF-19 uncovers a ciliary base-associated protein and a
832 CDK/CCRK/LF2p-related kinase required for intraflagellar transport. Dev. Biol. **357:** 235-
833 247.

834 Piasecki, B. P., T. A. Sasani, A. T. Lessenger, N. Huth and S. Farrell, 2017 MAPK-15 is a
835 ciliary protein required for PKD-2 localization and male mating behavior in *Caenorhabditis*
836 *elegans*. Cytoskeleton (Hoboken). **74:** 390-402.

837 Piasecki, B. P., J. Burghoorn and P. Swoboda, 2010 Regulatory factor X (RFX)-mediated
838 transcriptional rewiring of ciliary genes in animals. Proc. Natl. Acad. Sci. U. S.
839 A. **107:** 12969-12974.

840 Pyke, D. A., and J. N. Thompson, 1986 Statistical-analysis of survival and removal rate
841 experiments. Ecology **67:** 240-245.

842 Reith, W., and B. Mach, 2001 The bare lymphocyte syndrome and the regulation of MHC
843 expression. Annu. Rev. Immunol. **19:** 331-373.

844 Ruaud, A., I. Katic and J. Bessereau, 2011 Insulin/Insulin-like growth factor signaling
845 controls non-dauer developmental speed in the nematode *Caenorhabditis elegans*.
846 Genetics **187:** 337-343.

847 Saito, T. L., S. Hashimoto, S. G. Gu, J. J. Morton, M. Stadler *et al*, 2013 The transcription
848 start site landscape of *C. elegans*. Genome Res. **23:** 1348-1361.

849 Schackwitz, W. S., T. Inoue and J. H. Thomas, 1996 Chemosensory neurons function in
850 parallel to mediate a pheromone response in *C. elegans*. Neuron **17:** 719-728.

851 Schafer, J. C., C. J. Haycraft, J. H. Thomas, B. K. Yoder and P. Swoboda, 2003 XBX-1
852 encodes a dynein light intermediate chain required for retrograde intraflagellar transport and
853 cilia assembly in *Caenorhabditis elegans*. Mol. Biol. Cell **14:** 2057-2070.

854 Schroeder, N. E., R. J. Androwski, A. Rashid, H. Lee, J. Lee *et al*, 2013 Dauer-specific
855 dendrite arborization in *C. elegans* is regulated by KPC-1/Furin. Current Biology **23:** 1527-
856 1535.

857 Senti, G., and P. Swoboda, 2008 Distinct isoforms of the RFX transcription factor DAF-19
858 regulate ciliogenesis and maintenance of synaptic activity. Mol. Biol. Cell **19:** 5517-5528.

859 Senti, G., M. Ezcurra, J. Löbner, W. R. Schafer and P. Swoboda, 2009 Worms with a single
860 functional sensory cilium generate proper neuron-specific behavioral output.
861 Genetics **183:** 595-605.

862 Serrano-Saiz, E., R. J. Poole, T. Felton, F. Zhang, E. D. De La Cruz *et al*, 2013 Modular
863 control of glutamatergic neuronal identity in *C. elegans* by distinct homeodomain proteins.
864 Cell **155:** 659-673.

865 Shaye, D. D., and I. Greenwald, 2011 OrthoList: A compendium of *C. elegans* genes with
866 human orthologs. Plos One **6:** e20085.

867 Sieburth, D., Q. Ch'ng, M. Dybbs, M. Tavazoie, S. Kennedy *et al*, 2005 Systematic analysis
868 of genes required for synapse structure and function. Nature **436:** 510-517.

869 Slos, D., W. Sudhaus, L. Stevens, W. Bert and M. Blaxter, 2017 *Caenorhabiditis*
870 *monodelphis* sp. n.: Defining the stem morphology and genomics of the genus
871 *Caenorhabditis*. BMC Zoology **2**:4.

872 Starich, T. A., R. K. Herman, C. K. Kari, W. H. Yeh, W. S. Schackwitz *et al*, 1995 Mutations
873 affecting the chemosensory neurons of *Caenorhabditis elegans*. Genetics **139:** 171-188.

874 Su, J., H. Chiang, P. Tseng, W. Tai, C. Hsu *et al*, 2014 RFX-1-dependent activation of SHP-
875 1 inhibits STAT3 signaling in hepatocellular carcinoma cells. Carcinogenesis **35:** 2807-2814.

876 Sulston, J. E., E. Schierenberg, J. G. White and J. N. Thomson, 1983 The embryonic cell
877 lineage of the nematode *Caenorhabditis elegans*. Dev. Biol. **100:** 64-119.

878 Swoboda, P., H. T. Adler and J. H. Thomas, 2000 The RFX-type transcription factor DAF-19
879 regulates sensory neuron cilium formation in *C. elegans*. Mol. Cell **5:** 411-421.

880 Tammimies, K., A. Bieder, G. Lauter, D. Sugiaman-Trapman, R. Torchet *et al*, 2016 Ciliary
881 dyslexia candidate genes DYX1C1 and DCDC2 are regulated by regulatory factor X (RFX)
882 transcription factors through X-box promoter motifs. FASEB Journal **30:** 3578-3587.

883 Truong, T., Z. A. Karlinski, C. O'Hara, M. Cabe, H. Kim *et al*, 2015 Oxidative stress in
884 *Caenorhabditis elegans*: Protective effects of spartin. PloS one **10:** e0130455.

885 Tusher, V. G., R. Tibshirani and G. Chu, 2001 Significance analysis of microarrays applied
886 to the ionizing radiation response. Proc. Natl. Acad. Sci. U. S. A. **98:** 5116-5121.

887 Vayndorf, E. M., C. Scerbak, S. Hunter, J. R. Neuswanger, M. Toth *et al*, 2016
888 Morphological remodeling of *C. elegans* neurons during aging is modified by compromised
889 protein homeostasis. NPJ Aging and Mechanisms of Disease **2**: 16001.

890 Wang, J., H. T. Schwartz and M. M. Barr, 2010 Functional specialization of sensory cilia by
891 an RFX transcription factor isoform. Genetics **186:** 1295-1307.

892 Wu, Y., J. -. Zhang, T. Xu, L. Xu, J. Qiao *et al*, 2016 Identification of therapeutic targets for
893 childhood severe asthmatics with DNA microarray. Allergol. Immunopathol. **44:** 76-82.

894 Xie, Y., M. Moussaif, S. Choi, L. Xu and J. Y. Sze, 2013 RFX transcription factor DAF-19
895 regulates 5-HT and innate immune responses to pathogenic bacteria in *Caenorhabditis*
896 *elegans*. Plos Genetics **9:** e1003324.

FIGURE LEGENDS

Figure 1. *daf-19* structure and characterization of *daf-19(tm5562)* RNA products

A. Three promoters produce four related *daf-19* RNA products, as shown. Conserved DNA binding (DBD) and dimerization (DIM) domains are indicated above encoding exons; locations of a new deletion allele *tm5562* and the null allele *m86* are noted with brackets and arrows, respectively. **B.** Reverse transcription (RT) PCR using primers to exons 1 and 10 reveal a highly abundant 1123 bp *daf-19a* transcript from worms wild-type for *daf-19*, a 934 bp transcript from *tm5562* worms, and a much less abundant *daf-19b* product that is 75 bp larger. **C.** Sequencing trace from the smaller RT PCR product shows splicing of exon 3 to 5 as in *daf-19a*. **D.** Sequencing traces of exon 1 splicing in *daf-19a* cDNA products from wild-type N2 (top) and *daf-19(tm5562)* worms (below). **E.** Translated sequences from exon 2 of *daf-19* orthologs aligned using T-Coffee (Di Tommaso et al., 2011) and clustered (left) according to the phylogeny of Slos et al. (2017). Sequence IDs: *C. elegans* gi|71988112, *C. remanei* gb|EFP05251.1, *C. briggsae* emb|CAP22350.4, *C. sinica* scaffold 899, *C. brenneri* gb|EGT33833.1, *C. tropicalis* scaffold 563.1, *C. japonica* contig 15741.5, *C. angaria*, contig 57337_2.

Figure 2. Presence of DAF-19 activates expression of novel target genes in certain CSNs

Expression patterns of transcriptional fusions of *daf-19* target gene promoters with the GFP gene in isogenic *daf-12(sa204)* and *daf-19(m86); daf-12(sa204)* adult hermaphrodites (N=30 worms/strain analyzed). Views are lateral with dorsal at the top and anterior to the left, except strains expressing *eppl-1::gfp*. Neurons in which *daf-19*-dependent expression was

found are identified. Cell bodies in which gene expression is absent in *daf-19(m86)* mutants are indicated by dotted circles. Scale bar=10 μm.

Figure 3. DAF-19 presence down-regulates expression of novel target genes in certain non-sensory neurons and CSNs

Expression patterns of transcriptional fusions of *daf-19* target gene promoters with GFP in isogenic *daf-12(sa204)* and *daf-19(m86); daf-12(sa204)* adult hermaphrodites (N=30 worms/strain analyzed, except for *gakh-1*, N=130). Views are lateral with dorsal at the top and anterior to the left. Neurons in which *daf-19*-dependent expression was found are identified. Cell bodies in which gene expression is absent in worms wild-type for *daf-19* are indicated by dotted circles. Microvilli at the dendritic tips of AFD sensory neurons (in the right *skr-12* image) are magnified an additional 2x. Scale bar=10 μm.

Figure 4. *daf-19(tm5562)* confers decreased roaming behavior and aldicarb resistance

A. Each 1-day old adult worm roamed freely from the center of an OP50 bacterial lawn for one hour at 19°: shown are representative worm tracks for worms of indicated genotypes. **B.** Jitter plot of the proportion of grids crossed versus the total number of grids underneath the OP50 bacterial lawn; N=30 worms per assay. *tm5562 + a* indicates transgene expression of *daf-19a* from its endogenous promoter. The median and 1 SEM are indicated. Tukey's pairwise comparisons indicate that *tm5562* worms roam less than wild-type N2 worms on all assay dates ($p<0.003$), while *tm5562 + a* transgenic worms roam significantly more than *tm5562* worms ($p<0.03$). **C.** Response to 500 μM aldicarb was assessed as in Mahoney et al. (2006). Error bars are 1 SEM. Pair-wise comparisons of average paralysis curves (N=6

943 assays) were compared Peto and Peto (Pyke and Thompson, 1986). *tm5562* worms are not
944 different from *m86* worms (p=0.56), whereas *tm5562 + a* transgenic worms differ from *m86*
945 worms (p=0.02) and do not differ from wild-type N2 worms (p=0.56).
946
947 **Figure 5. Isoform-specific control of *daf-19* target genes**
948 **A.** Target genes activated by the presence of DAF-19 are still activated in a *daf-19(tm5562)*
949 background, where DAF-19C, but not DAF-19A is functional. These genes are also activated
950 when a transgene expressing DAF-19C, but not a DAF-19A transgene, is added to *daf-*
951 *19(m86)* null mutant worms. Over-expression of DAF-19A represses expression of *asic-2*,
952 *spg-20*, and *mapk-15* even in cells where expression is typically independent of *daf-19*
953 (Figure 2). N/A = expression of target gene in muscle prevented identification of *daf-19a* co-
954 injection marker. **B.** Two target genes, *skr-12* and *gakh-1*, are repressed in a *daf-19* wild-type
955 background, but are not repressed in a *daf-19(tm5562)* background when DAF-19A is non-
956 functional. Expression of *rgs-8.1* and *mapk-15* is repressed in the presence of either isoform
957 of DAF-19. Scale bar=10 μm.

SUPPLEMENTARY FIGURE AND TABLE LEGENDS

Figure S1. Tissue enrichment analysis of gene lists

Lists of genes differentially regulated by DAF-19 were analyzed using the WormBase (version WS258) Tissue Enrichment Analysis Tool, http://www.wormbase.org/tools/enrichment/tea/tea.cgi (Angeles-Albores et al., 2016). Nervous system cells/tissues are in blue font. *daf-19* regulated transcriptomes from 3-fold stage embryos (yellow), L1 larvae (red), and two-day old adults (blue) are compared; four-fold enrichment or greater is shown.

Figure S2. Identification of neurons in which *daf-19* target genes are expressed

Transcriptional fusions of *daf-19* target gene promoters with GFP were co-expressed with the indicated marker fusions (*promoter::mCherry*) or co-localized with fluorescent DiI. The expression of genes activated in the presence of DAF-19 is shown in wild-type adults. The expression of genes repressed in the presence of DAF-19 is shown in the *daf-19(m86)* null mutant genetic background. *eat-4* and *cho-1* promoter fusions are nuclear localized (gift from the Hobert lab). Scale bar=10 μm.

Figure S3. Expression patterns of genes (largely) independent of *daf-19*

Expression patterns of transcriptional fusions of putative *daf-19* target gene promoters with the GFP gene in *daf-12(sa204)* hermaphrodites. Images are typically lateral views with dorsal at the top and anterior to the left, except for images of the worm tail. Scale bar=10 μm

Figure S4. *daf-19(tm5562)* mutants lack phenotypes associated with *daf-19c*

A. Dauer formation assays performed in the presence of food and low population density demonstrate that *daf-19(tm5562*) is not dauer-constitutive (Daf-c). The proportion of dauer offspring produced by 20 gravid hermaphrodites at each temperature for wild-type N2 and *daf-19* mutant strains is shown. Error bars indicate 1 SD of 3 replicate assays. **B.** *daf-19(tm5562)* hermaphrodites dye-fill normally in the head (dorsal-ventral view) and in the tail (not shown). **C.** The development time of the L3 larval stage is slightly but significantly extended in *daf-19(tm5562)* mutant hermaphrodites compared to wild-type N2 ($p=0.00023$) at 48 hours of development. Error bars represent the 95% confidence interval, average replicate size=138 worms; results from three replicate assays are shown. **D.** *daf-19(tm5562)* is a hypomorphic or loss-of-function allele. Heterozygous *daf-19(tm5562/+)* animals display wild-type levels of aldicarb sensitivity. Response to 500 μM aldicarb was assessed as in Mahoney et al. (2006). Error bars are 1 SEM.

Table S1. *C. elegans* strains used in this study

Strains containing *daf-19* target transgenes or putative target transgenes are listed alphabetically by target gene name.

Table S2. Putative *daf-19* target genes generated from 3-fold stage embryo transcriptome

Gene list generated from comparative microarray analysis of transcriptomes from *daf-12(sa204)* versus *daf-19(m86); daf-12(sa204)* populations of 3-fold stage embryos. Data are reproduced, with permission, from Phirke et al. (2011).

Table S3. Putative *daf-19* target genes generated from L1 larvae transcriptome

Gene list generated from comparative microarray analysis of transcriptomes from *daf-12(sa204)* versus *daf-19(m86); daf-12(sa204)* populations of L1 larvae.

Table S4. Putative *daf-19* target genes generated from adult transcriptome

Gene list generated from comparative microarray analysis of transcriptomes from populations of two-day-old adult *daf-12(sa204)* versus *daf-19(m86); daf-12(sa204)* worms.

Table S5. Primers used to prepare target gene transcriptional fusions

Primers (5' to 3') used to prepare transcriptional fusions of candidate gene promoters with the GFP gene in Fire (pPD) vectors. Constructs include the ATG following the promoter region except that of C55B6.2, which stops 55 nucleotides upstream. K07C11.7 that includes 27 bases downstream, and C31A11.5 includes 22 bases of downstream sequence.

Table S6. Expression of gene transcriptional fusions (largely) independent of *daf-19*

Characteristics of *daf-19* independent genes and expression patterns of transcriptional fusions expressing soluble GFP are shown.

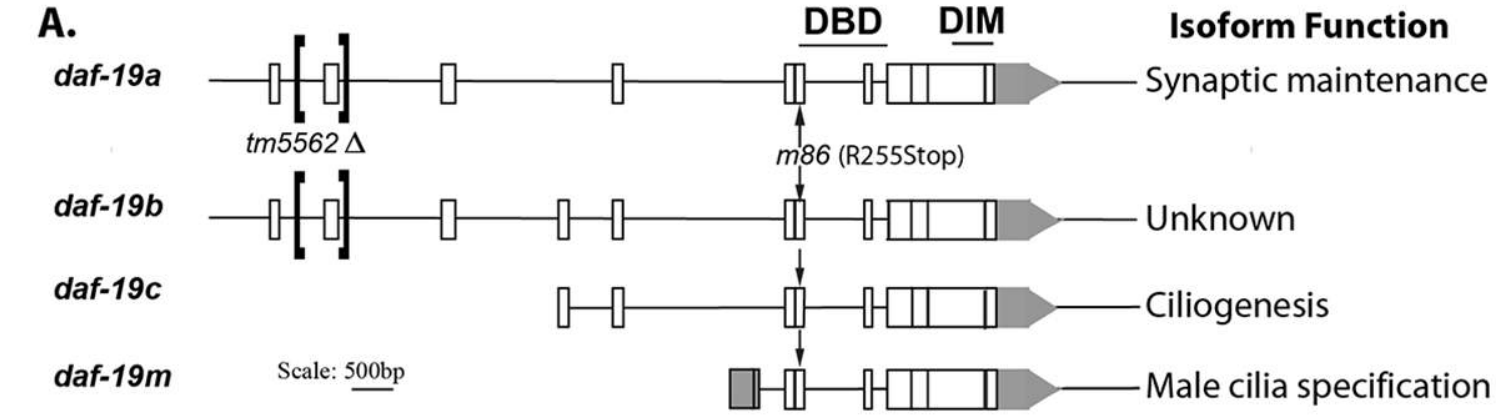
A.
DBD
DIM
Isoform Function
daf-19a
Synaptic maintenance
tm5562 Δ
m86 (R255Stop)
daf-19b
Unknown
daf-19c
Ciliogenesis
daf-19m
Scale: 500bp
Male cilia specification

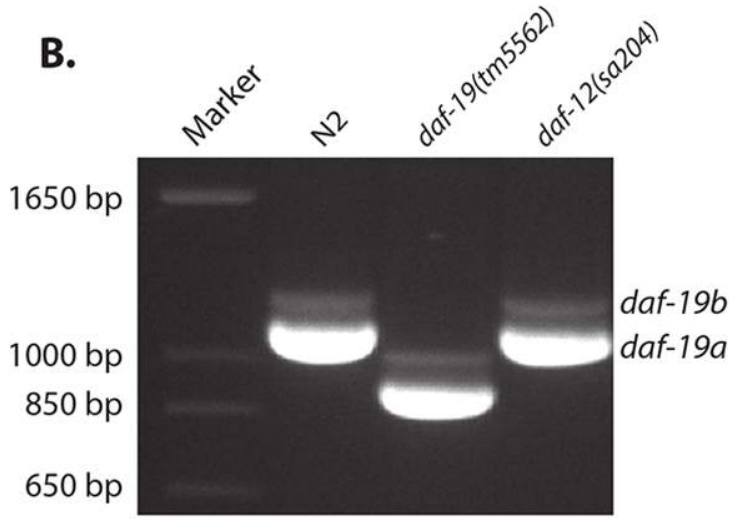
B.
Marker
N2
daf-19(tm5562)
daf-12(sa204)
1650 bp
1000 bp
850 bp
650 bp
daf-19b
daf-19a

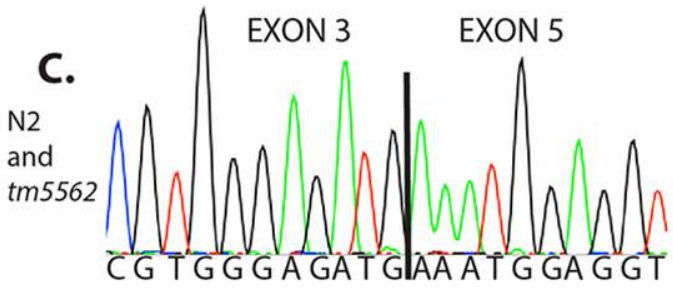
C.
N2
and
tm5562
EXON 3
EXON 5
C G T G G G A G A T G A A A T G G A G G T

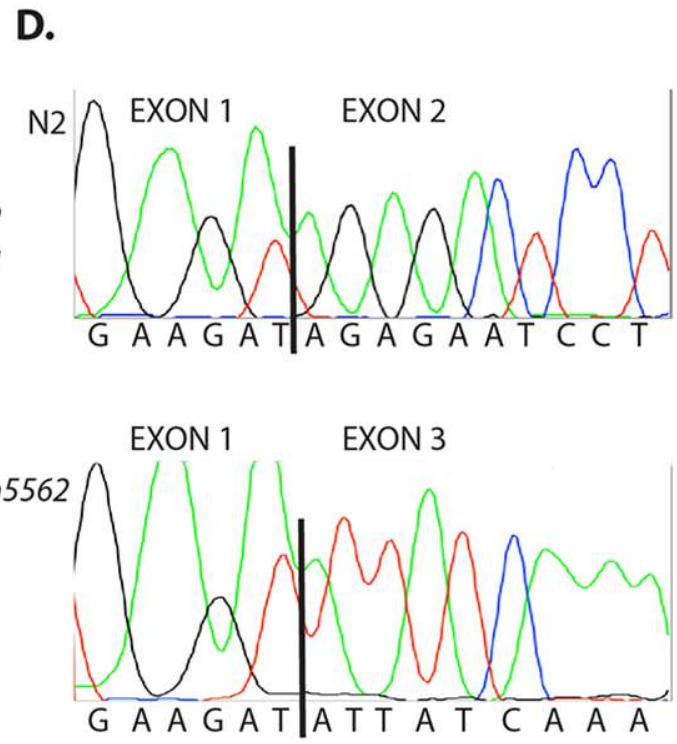
D.
N2
EXON 1
EXON 2
G A A G A T A G A G A A T C C T
tm5562
EXON 1
EXON 3
G A A G A T A T T A T C A A A

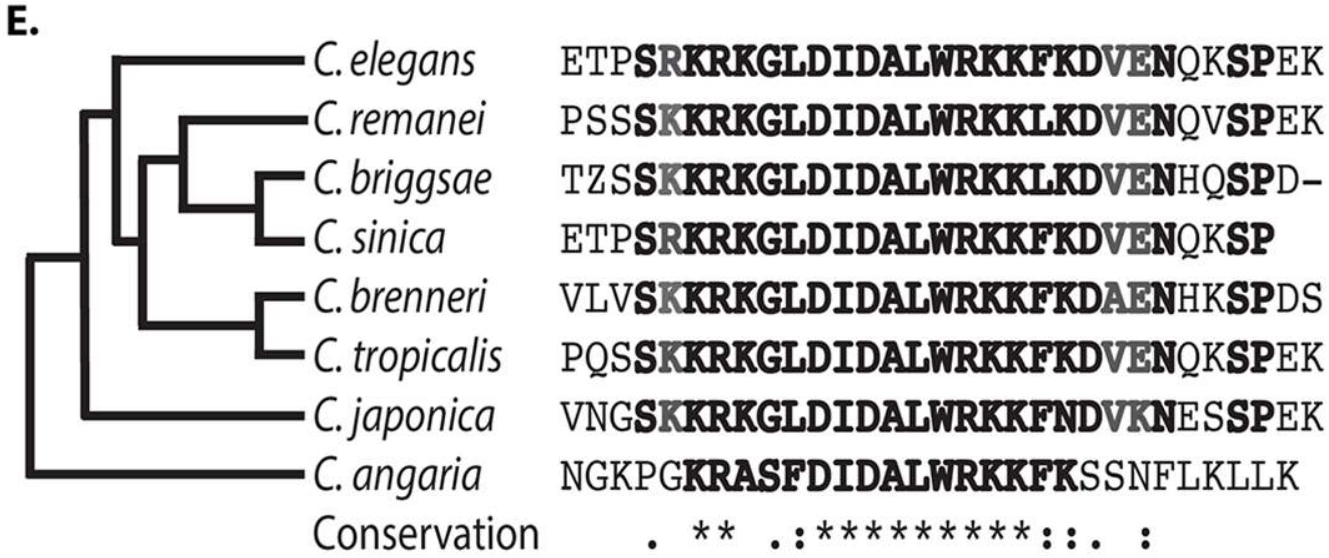
E.
C. elegans
C. remanei
C. briggsae
C. sinica
C. brenneri
C. tropicalis
C. japonica
C. angaria
Conservation
ETPSRKRKGLDIDALWRKKFKDVENQKSPEK
PSSSKKRKGLDIDALWRKKLKDVENQVSPEK
TZSSKKRKGLDIDALWRKKLKDVENHQSPD-
ETPSRKRKGLDIDALWRKKFKDVENQKSP
VLVSKKRKGLDIDALWRKKFKDAENHKSPDS
PQSSKKRKGLDIDALWRKKFKDVENQKSPEK
VNGSKKRKGLDIDALWRKKFNDVKNESSPEK
NGKPGKRASFDIDALWRKKFKSSNFLKLLK
. ** .:*********:. :

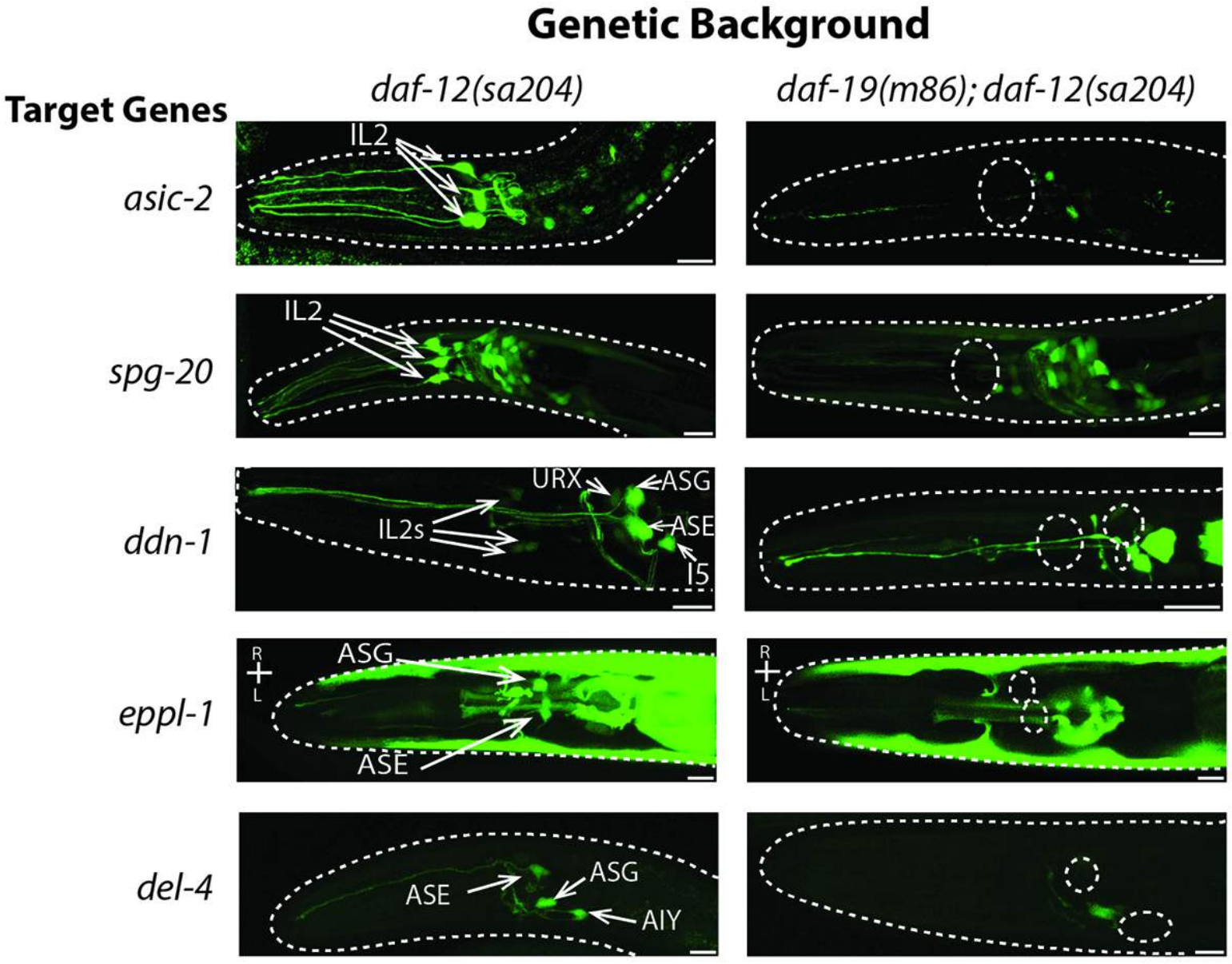
Genetic Background
Target Genes
daf-12(sa204)
daf-19(m86); daf-12(sa204)
asic-2
IL2
spg-20
IL2
ddn-1
URX
ASG
IL2s
ASE
I5
eppl-1
R
L
ASG
ASE
del-4
ASE
ASG
AIY

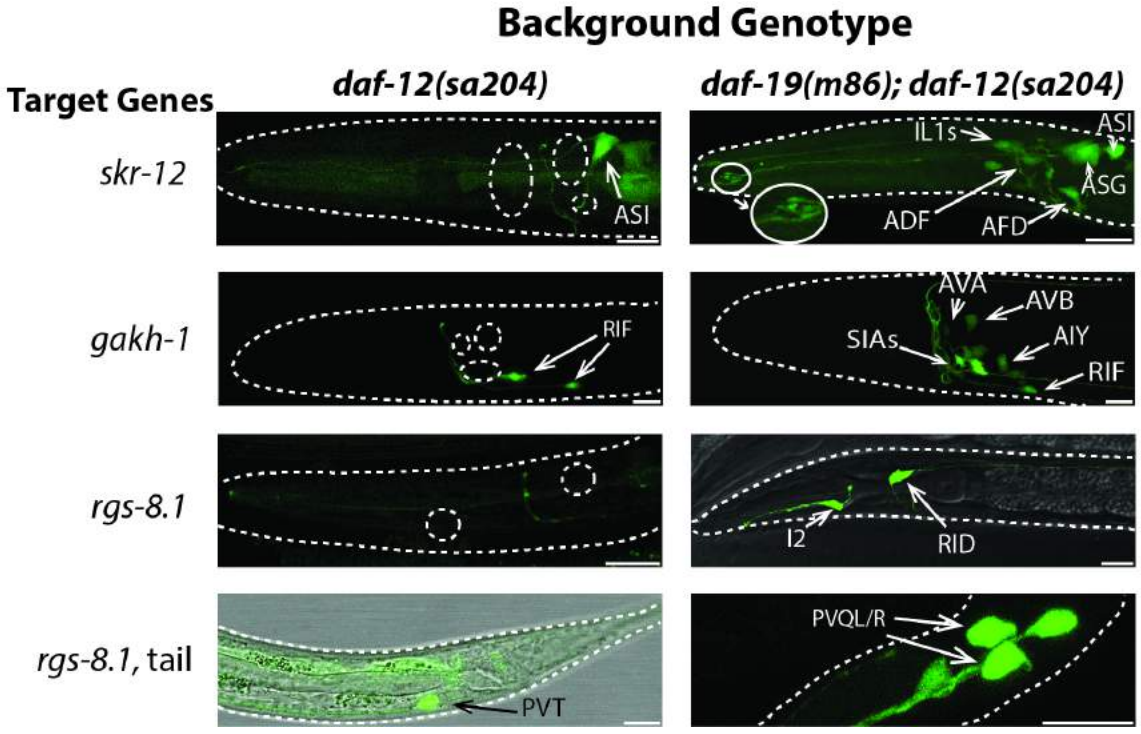
Background Genotype
Target Genes
daf-12(sa204)
daf-19(m86); daf-12(sa204)
skr-12
ASI
IL1s
ASI
ASG
ADF
AFD
gakh-1
RIF
AVA
AVB
SIAs
AIY
RIF
rgs-8.1
I2
RID
rgs-8.1, tail
PVT
PVQL/R

A.

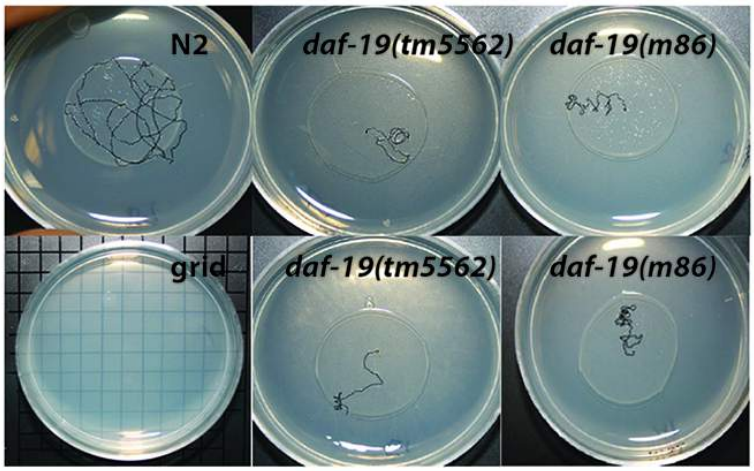
N2
daf-19(tm5562)
daf-19(m86)
grid
daf-19(tm5562)
daf-19(m86)

B.

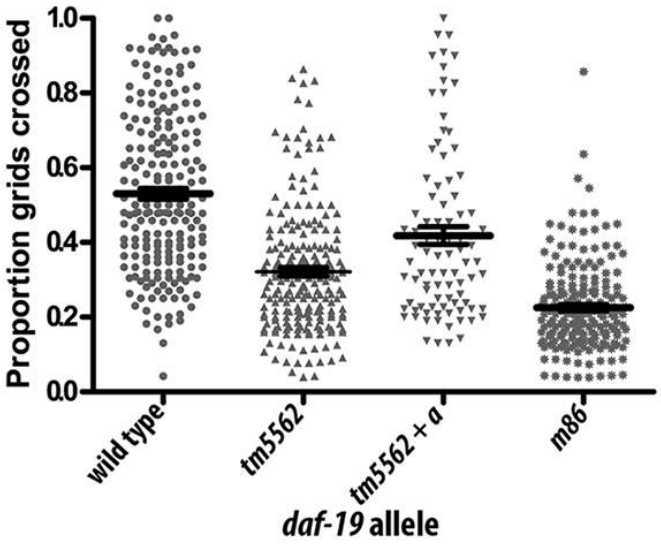
Proportion grids crossed
1.0
0.8
0.6
0.4
0.2
0.0
wild type
tm5562
tm5562 + a
m86
daf-19 allele

C.

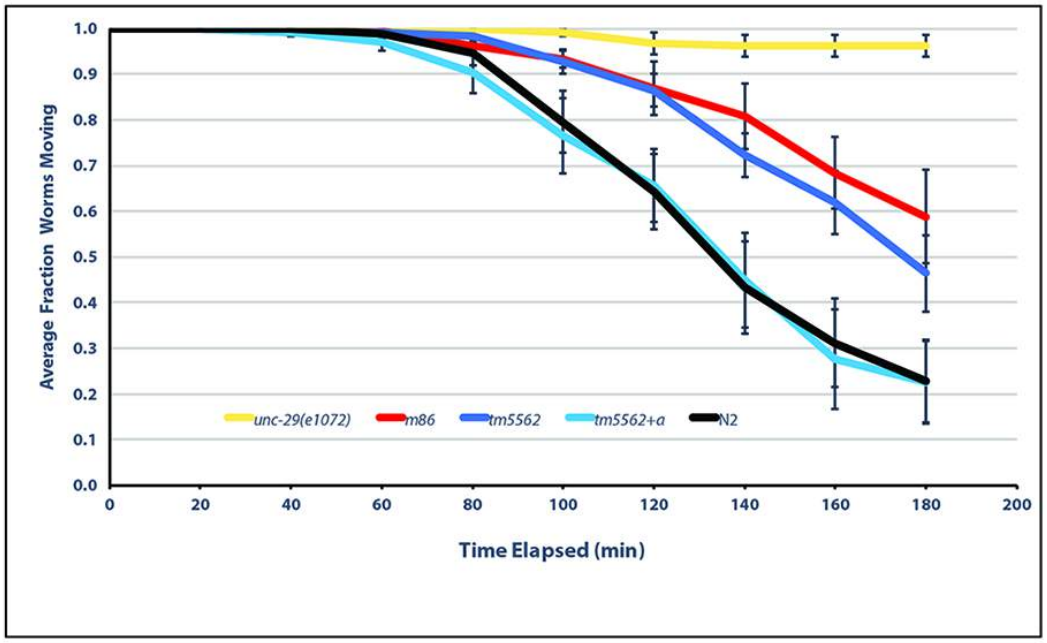
Average Fraction Worms Moving
1.0
0.9
0.8
0.7
0.6
0.5
0.4
0.3
0.2
0.1
0.0
unc-29(e1072)
m86
tm5562
tm5562+a
N2
0
20
40
60
80
100
120
140
160
180
200
Time Elapsed (min)

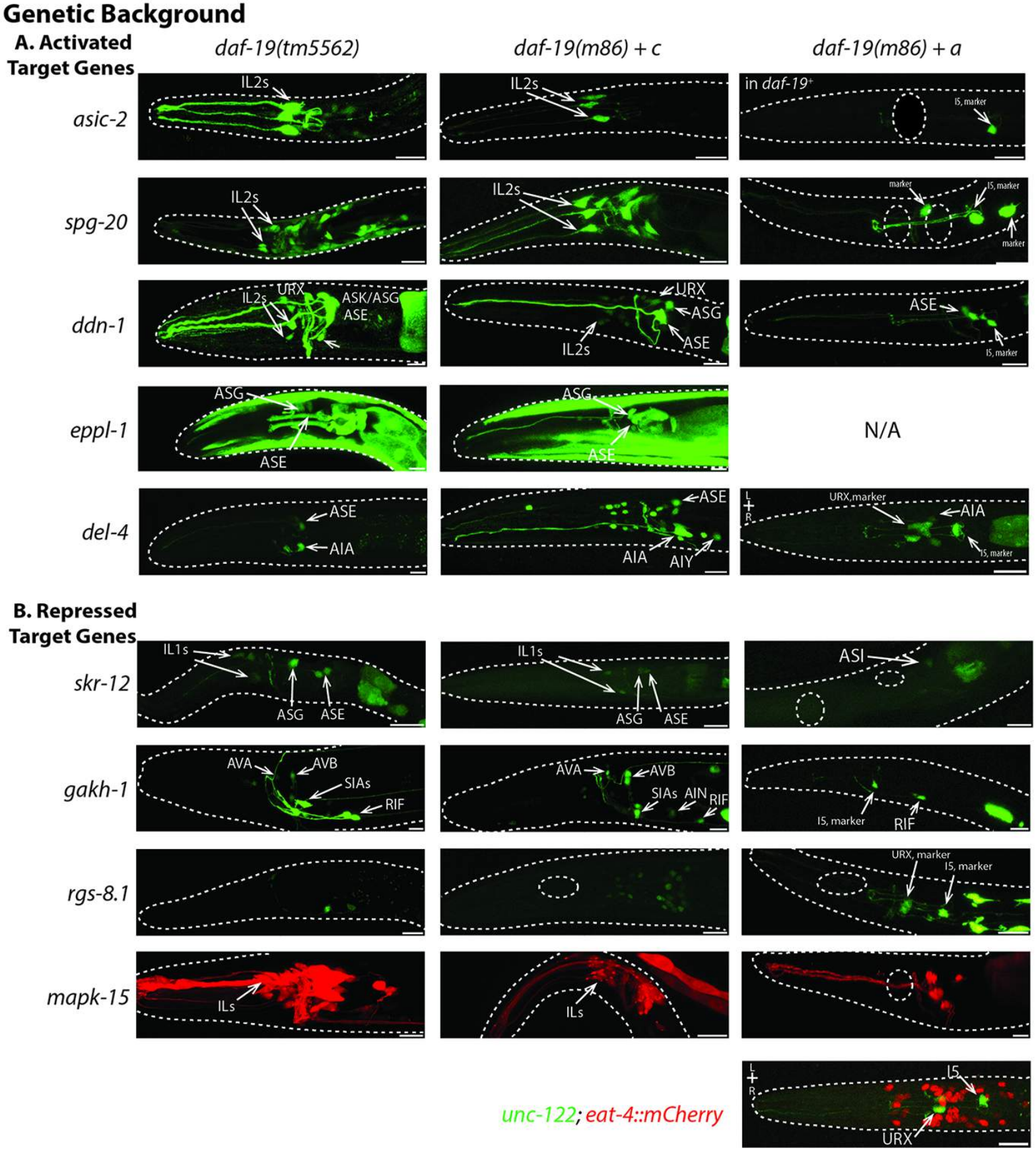
Genetic Background
A. Activated Target Genes
daf-19(tm5562)
daf-19(m86) + c
daf-19(m86) + a
asic-2
spg-20
ddn-1
eppl-1
del-4
B. Repressed Target Genes
skr-12
gakh-1
rgs-8.1
mapk-15
IL2s
URX
ASK/ASG
ASE
ASG
AIA
AIY
IL1s
AVA
AVB
SIAs
AIN
RIF
ILs
ASI
in daf-19+
I5, marker
marker
URX,marker
N/A
unc-122; eat-4::mCherry
L
R
I5